Fish and Shellfish Immunology 88 (2019) 284–292

Contents lists available at ScienceDirect

Fish and Shellfish Immunology

journal homepage: www.elsevier.com/locate/fsi

Full length article

Molecular cloning, characterization and expression analysis of S- adenosyl-L-homocysteine hydrolase (SAHH) during the pathogenic infection of *Litopenaeus vannamei* by *Vibrio alginolyticus*

QingJian Liang[a,b,c], MuFei Ou[a,b,c], YingHao Ren[a,b,c], ZeNa Yao[a,b,c], Rui Hu[a,b,c], JieZhen Li[a,b,c], Yuan Liu[a,b,c], Weina Wang[a,b,c,*]

[a] College of Life Science, South China Normal University, Guangzhou, 510631, PR China
[b] Key Laboratory of Ecology and Environmental Science in Guangdong Higher Education, PR China
[c] Guangzhou Key Laboratory of Subtropical Biodiversity and Biomonitoring, PR China

ARTICLE INFO

Keywords:
Litopenaeus vannamei
SAHH
Rack1
TLR

ABSTRACT

SAHH is an enzyme, playing a significant role in the catalyzation of the S-adenosyl homocysteine (SAH) into homocysteine (Hcy) and adenosine (Ado). However, little is known information of the enzyme in crustaceans. In the present study, SAHH cDNA was cloned from *Litopenaeus vannamei* (*LvSAHH*). The full length of the *LvSAHH* was found, containing a 5′ UTR of 119 bp, an ORF of 1236 bp and a 3′ UTR of 549 bp. The *Lv*SAHH gene encoded a polypeptide of 411 amino acids with an estimated molecular mass of 45.55 kD and a predicted isoelectronic point (pI) of 5.63. Comparison of the deduced amino acid sequence showed that *Lv*SAHH has high identity (70 %–82%) with other known species. qRT-PCR analysis revealed that *LvSAHH* mRNA was broadly expressed in all of the examined tissues, while the highest expression level was observed in muscle, followed by the expression in stomach, gill, pleopod, hepatopancreas, heart, eye and intestine. Subcellular localization analysis revealed that *Lv*SAHH was predominantly localized in the cytoplasm and nucleus. *LvSAHH* mRNA expression levels in hepatopancreas and gill were significantly up-regulated from 6 to 48 h after *V. alginolyticus* injection and reached the highest level (15-fold and 8-fold, $p < 0.01$) at 24 h, respectively. Additionally, the Toll-like receptors (*TLR*) and interleukins-16 (*IL-16*) were detected in hepatopancreas and gill of *LvSAHH*-knockdown SAHH. *LvRack1*, *LvToll1*, *LvToll2*, *LvToll3* and *LvIL-16* transcripts were decreased significantly in *LvSAHH*-knockdown shrimp at 24 h post *V. alginolyticus* stimulation in hepatopancreas and gill. But *LvToll3* was no significant difference in gill. In summary, these results indicated that *Lv*SAHH may play a regulatory role in the invertebrate innate immune defense by regulating *TLR* and *IL-16* expression.

1. Introduction

SAHH catalyzes the reversible hydrolysis of S-adenosyl homocysteine (SAH) to homocysteine (Hcy) and adenosine (Ado) in eukaryotes [1,2]. The reaction is reversible, and the equilibrium lies far in the direction of SAH synthesis. Under physiological conditions, the removal of both Ado and Hcy is sufficiently rapid that the net reaction proceeds in the direction of hydrolysis [3,4]. SAH is the product of all S-adenosylmethionine (SAM)-dependent biological transmethylations and acts as a potent inhibitor of SAM-dependent methyltransferases. Thus, the ratio of cellular SAH/SAM is frequently used as an indicator of cellular methylation status. The transmethylation reactions include methylations of proteins, lipids, nucleic acids, and small molecules are key factors in T and B cell immune responses in the development of inflammatory disease [5–8]. Inhibition of SAHH has been known to result in accumulation of intracellular levels of SAH, the immunosuppressive properties of SAHH inhibitors have been well known for years [9]. Previous studies showed that SAHH inhibitor DZ2002 has an immunomodulatory activity and to alleviate disease in several inflammatory and autoimmune animal models, by reducing pro-inflammatory cytokine production from macrophage and regulating TLR [9,10]. However, the knowledge of how SAHH regulates the gene expression of immune, as well as other target genes such as cytokines is still not very clear in invertebrates.

In *Drosophila melanogaster*, the Toll pathways are the major regulators of the immune response [11]. In shrimp, silencing *LvToll*

* Corresponding author. College of Life Sciences, South China Normal University, No.55 West Zhongshan Avenue, Guangzhou, Guangdong Province, 510631, PR China.
E-mail addresses: wangwn@scnu.edu.cn, weina63@aliyun.com (W. Wang).

https://doi.org/10.1016/j.fsi.2019.02.058
Received 26 November 2018; Received in revised form 22 February 2019; Accepted 25 February 2019
Available online 05 March 2019

Table 1
Summary of primers used in this study.

Names	Sequences (5'→3')		
For cDNA cloning			
*Lv*SAHH-5′GSP	CAGCCTGAAGGGCATTGATGGGGTC	*Lv*SAHH-5′NP	TCAGGTCACCGCCGTCGTC
*Lv*SAHH-3′GSP	CTGGCAAGACCTGTGTTGTGGCTGGC	*Lv*SAHH-3′NP	GGTGTGCACTTCCTGCCCAA
For real-time quantitative RT-PCR			
*Lv*SAHH-F	GCAAGACCTGTGTTGTGGCT	*Lv*SAHH-R	GTAACCCTCACAAGCAGCCTG
*Lv*Rack1-F	TGCTCTCCGTTGCTTTCAGT	*Lv*Rack1-R	TGGGGTTACTGTTGGAGGGA
*Lv*Toll1-F	TCGACCATCCCTTTTACACC	*Lv*Toll1-R	TTGCCTGGAAGGTCTGATTC
*Lv*Toll2-F	CATGCCTGCAGGACTGTTTA	*Lv*Toll2-R	GGCCTGAGGGTAAGGTCTTC
*Lv*Toll3-F	TCGTACAACCAGCTGACGAG	*Lv*Toll3-R	ATACTTCAGGTGGGCCACAG
*Lv*IL-16-F	AGCAAGAGCCTCGTGTCAGAC	*Lv*IL-16-R	TCCTCCAGAGAAAAGCCCAGT
β-actin-F	GCCCATCTACGAGGGATA	β-actin-R	GGTGGTCGTGAAGGTGTAA
For RNAi			
dsRNA-*Lv*SAHH-F	ATGACTTCCAAGCCAGCATACG	dsRNA-*Lv*SAHH-R	CGATAATGCTCTGGCTTGAAGG
dsRNA-GFP-F	ATGGTGAGCAAGGGCGAGGA	dsRNA-GFP-R	TTACTTGTACAGCTCGTCCA
dsRNA-*Lv*SAHH-T7-F	TAATACGACTCACTATAGGATGACTTCCAAGCCAGCATACG	dsRNA-*Lv*SAHH-T7-R	TAATACGACTCACTATAGGCGATAATGCTCTGGCTTGAAGG
dsRNA-GFP-T7-F	TAATACGACTCACTATAGGATGGTGAGCAAGGGCGAGGA	dsRNA-GFP-T7-R	TAATACGACTCACTATAGGTTACTTGTACAGCTCGTCCA
For protein expression			
pProEX-*Lv*SAHH-F	GGCGCCATGGATCCG**GAATTC**ATGACTTCCAAGCCAGCATACG		
pProEX-*Lv*SAHH-R	CGCCAAAACAGCCAAGCTT**GGTACC**ATAACGATAATGCTCTGGCTTGAAGG		
pGEX4T1-Rack1-F	CCGCGTGGATCCCCG**GAATTC**ATGAATGAGAGCTTACAGCTGCG		
pGEX4T1-Rack1-R	GTCACGATGCGGCC**GCTCGAGC**GCACGGGAAGTAACGATGAC		
pFBDM-SAHH-F	GGTCCGAAGCGCGCG**GAATTC**ACATCAAAATGGCGGAGAAGGAGATGC		
pFBDM-SAHH-R	CTAGTACTTCTCGAC**AAGCTT**CTTATCGTCGTCATCCTTGTAATCATAACGATAATGCTCTGGCTTGAAGG		
pFBDM-Rack1-F	TTGATCACCCGGGAT**CTCGAG**TGATCAAAATGAATGAGAGCTTACAGCTGCG		
pFBDM-Rack1-R	GCCTCCCCCATCTCCC**GGTACC**TTACAGATCCTCTTCAGAGATGAGTTTCTGCTCCGCACGGGAAGTAACGATGAC		
For subcellular localization			
pAC5.1-*Lv*SAHH-GFP-F	TCTAATCCAGAGACCCCGGATCGG**GGTACCATCAAA**ATGGCGGAGAAGGAGATGC		
pAC5.1-LvSAHH-GFP-R	TCACGCTACTAGCCATGAATT**CCACCACACTGG**CATAACGATAATGCTCTGGCTTGAAGG		

a Nucleotides in bold indicate restriction sites introduced for cloning and underlined was label.
b The Kozak translation initiation sequence is shown in bold and in a box.
c The T7 RNA polymerase binding site is underlined.

increased mortality and reduced pathogen clearance after *Vibrio harveyi* challenge [12]. *Fc*Toll and *Mj*Toll are responsive to various immune challenges [13,14]. Interleukins play essential roles in regulation of various innate and adaptive immune processes. Interesting, Rack1 plays an important role in innate immune response in invertebrates [15]. It can functionally interact with immune-related cytokine and anti-virus protein, such as interleukin-3 (*IL-3*), *IL-5* and granulocyte macrophage colony stimulating factor [16], interferon receptor [17]. These expression pattern of SAHH and Rack1 in response stress has a potential link with organism's immune response.

Litopenaeus vannamei is an economically important species of shrimp aquaculture worldwide [18,19]. Environmental stress factors may affect the ability to maintain homeostasis and the metabolism, growth, survival, osmotic capacity and immune system of *Litopenaeus vannamei* [20,21]. Therefore, understanding the innate immune system of shrimp might contribute to developing strategies for the prevention and treatment of these diseases.

SAHH has been isolated and cloned from a variety of sources, such as bacteria, parasites, plants, amphioxus, mouse, rat, porcine, human. But there is little information of the enzyme about crustaceans. We found that SAHH has a significant difference in the transcriptome after *L. vannamei* being treated in different stress (*Vibrio alginolyticus* and temperature). We hypothesized that SAHH activities in overall stress mitigation may offer insights into general adaptive and defense responses in *L. vannamei*. In this study, we reported SAHH gene and its molecular properties, phylogenetic relationship and identified its regulates mechanism related to immune in response to low temperature stress. These findings would be helpful for understanding the activation mechanism of SAHH as well as its function in regulating the production of cytokines in invertebrate.

2. Materials and methods

2.1. Animals

L. vannamei, 6.86 ± 0.39 cm long and weighing 3.03 ± 0.53 g, were collected from a local shrimp farm in Panyu (Guangdong, China) and reared in 20 m^3 cycling filtered fiberglass tanks in which the salinity (5‰) and temperature (25 ± 2 °C) were maintained at the same levels as in standard shrimp culture ponds. Prior to experimental use, animals were acclimated to the laboratory conditions for 1 week, and fed three times per day with commercial shrimp feed until 24 h before the experimental treatments began, when feeding ceased.

2.2. Challenge experiment

Immune challenge experiments were performed to determine the *Lv*SAHH expression profiles of infected and control shrimp. *V. alginolyticus* (ATCC33787) was suspended in 1 × PBS (pH 7.2) with concentration of 10^7 CFU/ml. Thirty shrimps were randomly transferred to plastic aquaria for each group. One group received a 10 μL intramuscular injection of the *V. alginolyticus* dilution at the fourth abdominal segment, while another group was injected with 10 μL PBS at the same site for negative control. Three shrimp from each group were then randomly selected for hepatopancreas and gill collection at 0, 3, 6, 12 and 24 h post-challenge. The cDNA synthesis and RT-qPCR were performed as described above. Each treatment was replicated three times.

2.3. RNA extraction and cDNA synthesis

Total RNA was then extracted from the samples, using Trizol (Invitrogen, USA) following the manufacturer's instructions for quantitative real-time PCR (qPCR). The purity of the RNA samples was verified by measuring their absorbance at 260 and 280 nm using NanoDrop 2000 (USA) and its integrity was confirmed by 1.2% agarose

electrophoresis. First-strand cDNA was synthesized with total RNA 1 μg in each reaction systems using PrimeScript RT reagent Kit With gDNA Eraser (Takara, Dalian, China) according to the manufacturer's protocol. Rapid amplification of cDNA ends (5′, 3′ RACE) was accomplished using a BD SMART RACE cDNA amplification kit (BD Bioscience Clontech, CA, USA) following the manufacturer's instructions.

2.4. Bioinformatics analysis

According to the highly-conserved domains of SAHH sequence from other species in the GenBank database (http://www.ncbi.nlm.nih.gov/genbank/), a partial sequence of *Lv*SAHH was obtained by the touchdown PCR using the degenerate primers (Table 1), and the liver cDNA was used as the template. Both the nucleotide sequence and the amino acid sequence of *Lv*SAHH and/or *Lv*SAHH were analyzed on NCBI blast program (http://www.ncbi.nlm.nih.gov/blast/Blast.cgi). The conserved domain of *Lv*SAHH sequence was predicted by the motif scan analysis program (http://myhits.isb-sib.ch/cgi-bin/motif_scan). The multiple sequence alignments of the *Lv*SAHH amino acid were conducted by using the BioEdit. The phylogenetic tree was constructed using the neighbor-joining (NJ) method within MEGA software (version 7.0).

2.5. Quantitative real-time PCR analyses

cDNA was prepared from the samples collected from shrimp challenged with dsRNAs and *V. alginolyticus*. Differential expression analysis was performed using an ABI 7500 Real-Time PCR system (Applied Biosystems, USA). The PCR reactions were conducted in a volume of 20 μL comprising 10 μL of SYBR Premix Ex Taq™II (TaKaRa, Japan), 6.8 μL of sterile distilled water, 0.4 μL of each primer (10 μM), 0.4 μL of ROX Reference Dye (50 ×) and 2 μL of 1:20 diluted cDNA. Triplicate analyses were performed for each sample. The PCR program were 95 °C for 30 s, 40 cycles of 95 °C for 15 s, 60 °C for 30 s, and 72 °C for 30 s. Melting curve analysis was implemented at the end of the qRTPCR to confirm the credibility. The results were then determined by $2^{-\triangle\triangle Ct}$ methods. The primers used are shown in Table 1.

2.6. Expression purification of the recombinant LvSAHH protein and polyclonal antibody preparation

Briefly, *LvSAHH* ORF cDNA was subcloned between the *Eco*RI and *Hin*dIII sites of the pProEX-SAHH vector with Trelief ™ SoSoo Cloning Kit Ver.2 (Tsingke, BeiJing, China) following the manufacturer's recommendations. pProEX-SAHH vector was transformed into *E. coli* BL21, and the success of the ligation was confirmed by sequencing. The recombinant *Lv*SAHH was then over-expressed in *E. coli* BL21 cells by induction with isopropyl-β-thiogalactopyranoside (IPTG). After incubation at 37 °C for a further 3 h, the bacterial cells were harvested by centrifugation at 8000 × *g* for 10 min at 4 °C, re-suspended in 50 mM phosphate buffered solution (PBS, pH 8.0) containing 0.3 M NaCl and 10 mM imidazole, and sonicated on ice. The cell debris was removed by centrifugation at 15,000 × *g* for 20 min, and the supernatant was collected. The recombinant *Lv*SAHH was then purified using a glutathione sepharose 4B affinity chromatography system from Amersham Pharmacia Biotech (Piscataway, NJ, USA) following the manufacturer's protocol [22]. The purified recombinant *Lv*SAHH was used for analysis by SDS-PAGE and protein concentrations were determined by the method of Bradford.

The purified recombinant *Lv*SAHH was used to raise antibodies in a New Zealand white rabbit by emulsifying approximately 1 mg of the purified *Lv*SAHH with Freund's complete adjuvant and injecting it subcutaneously at multiple sites of the rabbit. Three booster injections of 1.5 mg antigen (0.5 mg each time) mixed with Freund's incomplete adjuvant were subsequently administered subcutaneously at intervals of 3 weeks. Six days after the final booster, blood was collected and serum was prepared. Serum from the same rabbit collected prior to immunization was used as a control. The anti-sera were aliquoted and stored at −80 °C.

2.7. Cell culture and subcellular localization

Drosophila S2 cells were grown in Schwartz Differential Medium (SDM) supplemented with 10% heat-inactivated fetal bovine serum (FBS; GIBCO, USA) and penicillin (100 IU/ml)/streptomycin (100 mg/ml). Cultures were maintained at 28 °C in cell culture incubator. An Endotoxin-free Plasmid Maxiprep Kit were used plasmid purification (Omega, USA) following the manufacturer's recommendations. For a transient transfection experiment, S2 cells were transfected with the indicated expression plasmids by using Escort ™ IV transfection reagent (Sigma, Germany) according to the manufacturer's protocol. Transfected S2 cells were incubated for 24 h in 24-well plate, then washed with PBS three times, stained with 50 nM Mito-Tracker (Beyotime, China) working solution at 27 °C for 40 min. And then washed with PBS three times, fixed with 4% paraformaldehyde, and stained with DAPI (1 μg/ml). Fluorescence was detected using a confocal laser scanning microscope (LSM 710, Zeiss, Germany).

2.8. GST pull-down

S2 cells were grown in 6-well plate for 18 h. Cells were transfected with pAC5.1-SAHH plasmid and cultured with fresh medium, harvested and lysed at 36 h post-transfection. Supernatant of cell lysates was incubated with the above purified GST/GST-Rack1 coupled with GST beads at 4 °C. Then, beads were washed with 1% Triton X-100/PBS three times and then eluted. After that, proteins were loaded on 12% SDS-PAGE gels, ectrophoretically separated, transferred to Bio-rad PVDF membranes on ice at 250 mA for 90 min, washed in TBST for 5 min and then incubated with blocking buffer containing 5% BSA for 1 h, followed by incubation with 1:500 diluted anti-GST antibody and anti-SAHH antibody at 4 °C overnight. The PVDF membranes were washed in TBST, incubated with 1:2000 diluted peroxidase-conjugated antibody for 60 min at room temperature. Following three times washes in TBST, PVDF membranes were developed and visualized. The experiment was performed in triplicate.

2.9. Coimmunoprecipitation

$LvSAHH_{Flag}$ cDNA was subcloned between the *Eco*RI and *Hin*dIII sites of the pFBDM vector with Trelief ™ SoSoo Cloning Kit Ver.2, pFBDM-SAHH was transfection into *E. coli* BL21, And then pFBDM-SAHH vector were used purification with Plasmid Kit, then, $LvRack1_{Myc}$ cDNA was subcloned between the *Kpn*I and *Xho*I sites of the Pfbdm-SAHH vector with Trelief™ SoSoo Cloning Kit Ver.2, construction pFBDM-$SAHH_{Flag}$-$Rack1_{Myc}$ vector. S2 cells transfected with pFBDM-$SAHH_{Flag}$-$Rack1_{Myc}$ or pFBDM at 48 h were harvested and then cells were lysed in 300 μl in 6-well plate with the lysis buffer (50 mM Tris-HCl, pH 8.0, 100 mM NaCl, 5 mM EDTA, 0.5% Triton X-100, and 1 mM PMSF). The soluble supernatants were mixed with the anti-Flag or the anti-Myc antibody, and incubated for 2 h at 4 °C. Protein G-Sepharose beads were then added and incubated for 1 h at 4 °C. The samples were washed with the lysis buffer three times and the bound proteins were eluted by boiling in the SDS-sample buffer. Proteins were analyzed by 10% SDS-PAGE, the gels were washed in TBST (50 mM Tris-HCl (pH 7.4), 2.5 M NaCl, 0.05% Tween-20) for 10 min, and the separated proteins were transferred to PVDF membranes on ice at 100 V for 90 min. Then, membranes were washed in TBST for 5 min, and incubated in 20 mM TBS (50 mM Tris-HCl (pH 7.4), 2.5 M NaCl) containing 3% BSA at 4 °C overnight. The membranes were then washed in TBST for 5 min, and incubated with the anti-Rack1 (Beyotime, China) and anti-Myc (Beyotime, China) or anti-SAHH and anti-Flag (Beyotime, China) primary antibody diluted 1:1000 in 0.5% BSA-TBST for

60 min at room temperature with gentle shaking. Following four washes in TBST (10 min per wash), the membranes were incubated with the peroxidase-conjugated secondary antibody diluted 1:2000 for 60 min at room temperature. Following a further four 10 min washes in TBST, the membranes were visualized with ECL detection reagents (Beyotime, China) using a DAB imaging analysis system (Bio-Rad, USA).

2.10. RNA interference

The cDNA fragment of *LvSAHH* was amplified by the primers *Lv*SAHH-Fi and *Lv*SAHH -Ri linked to the T7 promoter (Table 1), and used as template to synthesize dsRNA of *LvSAHH*. *dsGFP* was used as control and amplified with primers GFP-Fi and GFP-Ri (Table 1). dsRNA was synthesized using T7 RiboMAX Express (Promega, USA) according to the manufacturer's protocol. *L.vannamei* were separated into two groups and intramuscularly injected with either *dsLvSAHH* (2.5 μg/g shrimp) or *dsGFP* (2.5 μg/g shrimp) at the fourth abdominal segment. After 36 h both groups (designated *GFP* and *LvSAHH*, respectively) were injection *V. alginolyticus*. Samples were collected after 0, 3, 6, 12 and 24 h, the hepatopancreas and gill of three shrimps of each group were collected and separately frozen in liquid nitrogen for RNA extraction.

2.11. Statistical analyses

We used SPSS (version 20.0 for Windows) for all statistical analyses and considered $p < 0.05$ (*) or $p < 0.01$ (**) as significant for all statistical tests. Significant differences of the bacterial abundance across different treatments were analyzed by performing one-way ANOVA. All results are expressed as means ± *SD*. Non-normally distributed data were transformed to natural logarithms. Differences among groups were analyzed with one-way ANOVA followed by LSD post hoc comparisons.

3. Results

3.1. Characterization of LvSAHH

The full-length *LvSAHH* cDNA was 1664 bp, containing a 5′ UTR of 119 bp, an ORF of 1236 bp and a 3′ UTR of 549 bp (Fig. 1). The ORF putatively encodes a polypeptide of 411 amino acids with an estimated molecular mass of 45.55 kDa and a predicted isoelectric point (pI) of 5.63. The deduced amino acid sequence of *Lv*SAHH was compared with the sequences of SAHH from other species that were available in GenBank, and submitted to the NCBI GenBank under accession number JN676157. The BLAST (blastp) search of the NCBI database with the deduced amino acid sequence for S-adenosylhomocysteine hydrolase from *L.vannamei* revealed that *Lv*SAHH had the highest similarity (82%) to *Anopheles gambiae*, and shared 70 %–81% similarity to other known SAHH sequences (Fig. 2).

A phylogenetic tree, based on the deduced amino acid sequences from the different SAHH of 17 known species, was created using the neighbor-joining (NJ) method to determine the position of the *Lv*SAHH in an evolutionary context. Phylogenetic analysis showed that *Lv*SAHH and from the other insects, were grouped into one cluster (Fig. 3).

3.2. Expression of recombinant LvSAHH and polyclonal antibody preparation

An expression vector pProEX HT-b, including the entire ORF of *Lv*SAHH, was constructed and transformed into *E. coli* BL21, following which the recombinant *Lv*SAHH was purified by affinity chromatography. The purified recombinant *Lv*SAHH with the His-tag yielded a single band of 49 kDa on SDS-PAGE gels after Coomassie blue staining (Fig. 4a). Rabbit antiserum was obtained against the purified recombinant *Lv*SAHH with a rate of 1:600, which reacted in Western blot analysis with a constituent (apparent molecular weight, 49 kDa) of the

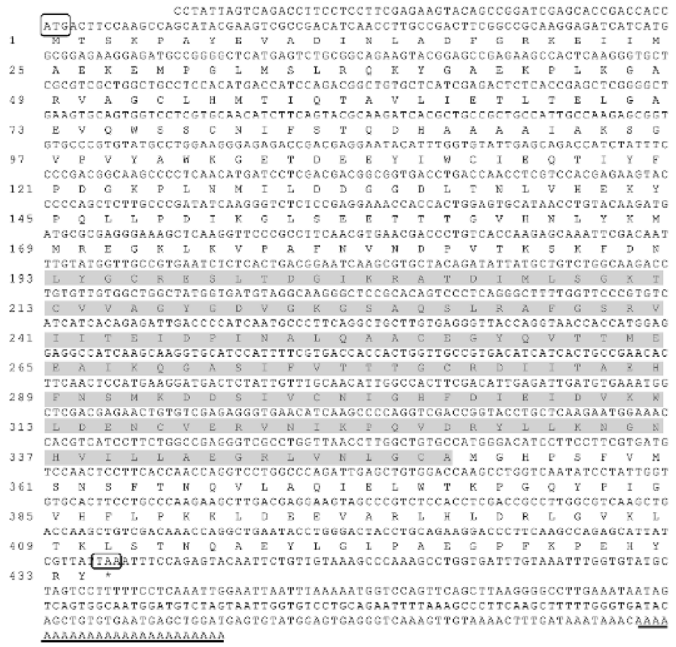

Fig. 1. Nucleotide and deduced amino acid sequences of *Lv*SAHH (Genbank accession No. JN676157). The initiation codon (ATG) and stop codon (TAA) were boxed, respectively. The potential poly adenylation signal (ATTAAA) and the ploy (A) tail were underlined, respectively. The NAD binding domain was shaded in gray.

supernatant of the cell lysate of IPTG-induced *E. coli* BL21 carrying the expression vector, but not with any constituents of a corresponding preparation of *E. coli* BL21 containing the expression vector prior to induction by IPTG. The antiserum was also reactive with a constituent that had an apparent molecular weight ca. 49 kDa, corresponding to the molecular mass predicted for *Lv*SAHH cDNA of the shrimp hepatopancreas homogenates (Fig. 4b). These findings show that the rabbit antiserum had marked antigen-specific reactivity.

3.3. Subcellular localization and tissue-specific expression

Subcellular localization was a dominant functional characteristic and tightly linked with its function. To determine the subcellular localization of *Lv*SAHH was determined by pAc5.1-GFP-*Lv*SAHH fusion protein assay. The result shown that the green fluorescence signaling was observed throughout the cytoplasm and nucleus in pAc5.1-GFP transfected cells, but the green fluorescence signaling was also aggregated in the cytoplasm and nucleus in pAc5.1-*Lv*SAHH-GFP transfected cells (Fig. 5a). A strong *Lv*SAHH mRNA or protein expression was detected in *Lv*SAHH overexpression cells at 36 h post transfection by using PCR or LvSAHH antiserum (Fig. 5b).

The expression of *LvSAHH* mRNA was detected by RT-PCR in heart, hepatopancreas, stomach, intestine, gill, eye, pleopod and muscle tissues (Fig. 5c). β-actin was as an internal control. The results showed that *LvSAHH* mRNA was expressed in almost all examined tissue types, but they were especially higher in hepatopancreas and stomach, and was detected at lower levels in the other tissues. These results suggest that *LvSAHH* was differentially expressed in different tissues.

3.4. Specific interaction of Rack1 and SAHH in vitro and in vivo

It has been reported that Rack1 plays an important role in the intracellular signaling of resistance to apoptosis induced by contaminants [23]. To further confirm the protein-protein interaction of SAHH with Rack1, *in vitro* binding assays were performed. We constructed a glutathione S-transferase (GST) and GST-Rack1 fusion protein.

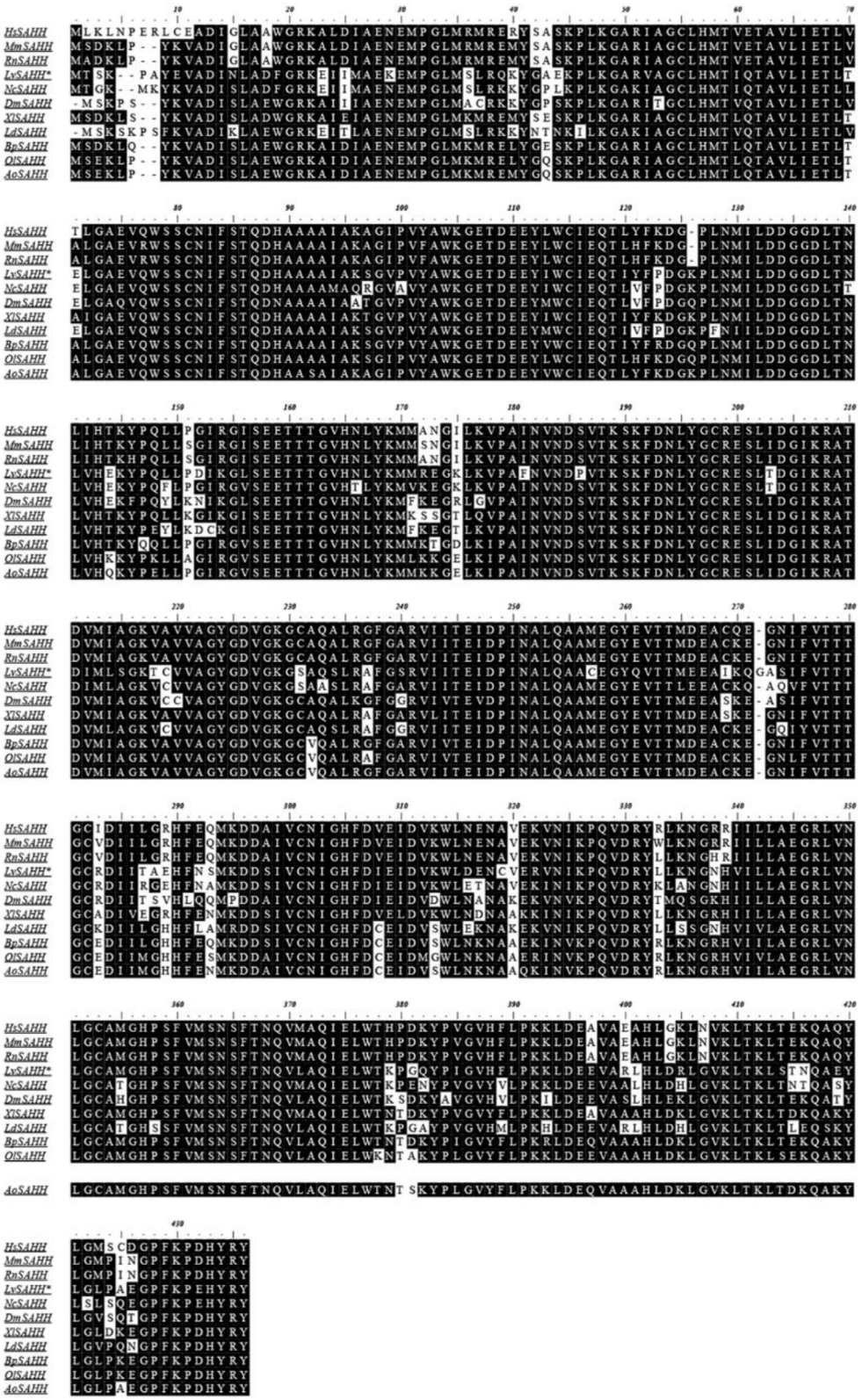

Fig. 2. Multiple sequence alignment of the deduced amino acid of *Lv*SAHH with other SAHH. The shared residues represented the similar regions between the different species, and the conservative degree was distinguished from light to dark.

Overexpressed SAHH in S2 cell was incubated with GST, or GST-Rack1 immobilized onto glutathione-Sepharose beads. The beads were washed with binding buffer three times, and GST or GST-Rack1 bound proteins were eluted with 2 × SDS sample buffer. Following separated on 10% SDS-PAGE, the bound proteins were analyzed by ECL method. Our findings suggest that SAHH bound to GST-Rack1 but not to GST, indicating that SAHH can interact with Rack1 (Fig. 6a).

To examine whether SAHH could interact with Rack1 *in vivo*, S2 cells were transiently transfected with the expression plasmid encoding Flag-SAHH and Myc-Rack1, which was designed to express full-length

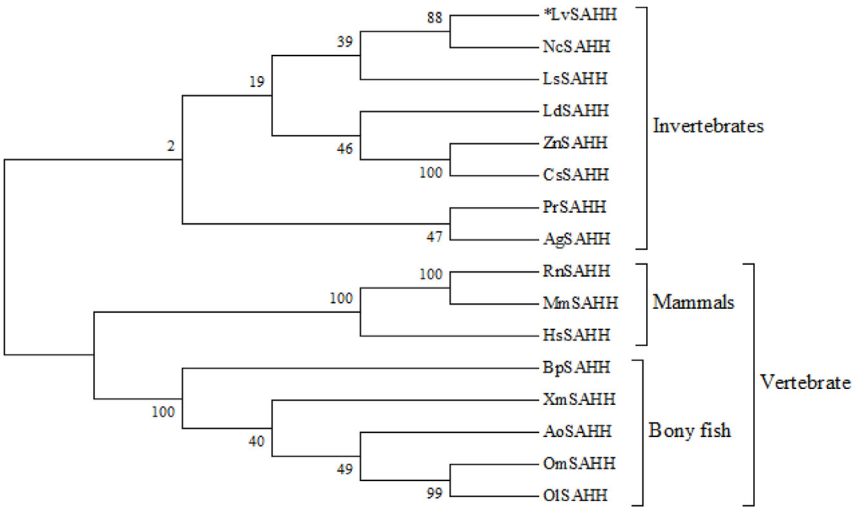

Fig. 3. A phylogenetic tree of *Lv*SAHH with 17 other SAHH species reconstructed using the NJ method. The tree is based on an alignment corresponding to full-length sequences by Mega 7.0 with 1000 bootstrap replications. The GenBank accession numbers for the sequence designations are as follows: *Hs*SAHH (*Homo sapiens*, NP_000678); *Rn*SAHH (*Rattus norvegicus*, NP_058897.1); *Mm*SAHH (*Mus musculus*, EDL06108); *Xl*SAHH (*Xenopus laevis*, NP_001089027); *Bp*SAHH (*Boleophthalmus pectinirostris*, XP_020786066.1); *Xm*SAHH (*Xiphophorus maculatus*, XP_023180569.1); *Ao*SAHH (*Amphiprion ocellaris*, XP_023154575.1); *Ol*SAHH (*Oryzias latipes*, XP_004069107.3); *Om*SAHH (*Oryzias melastigma*, XP_024125950.1); *Nc*SAHH (*Nephila clavipes*, PRD24306.1); *Ls*SAHH (*Lepeophtheirus salmonis*, ADD38615.1); *Ld*SAHH (*Leptinotarsa decemlineata*, XP_023018187.1); *Zn*SAHH (*Zootermopsis nevadensis*, XP_021933308.1); *Cs*SAHH (*Cryptotermes_secundus*, XP_023717501.1); *Ag*SAHH (*Anopheles gambiae*, AAC29475.1); *Pr*SAHH (*Pieris rapae*, ASJ26447.1).

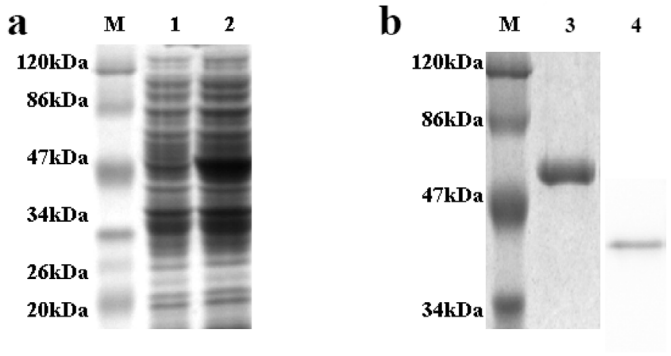

Fig. 4. Expression and purification of the recombinant *Lv*SAHH fusion protein. M, Prestained protein size markers (Fermentas); 1, vector control from BL21; 2, crude extract from BL21 induced with 1 mM IPTG. 3. Purification of the recombinant *Lv*SAHH fusion protein; 4. Western blotting with anti-*Lv*SAHH polyclonal antibody.

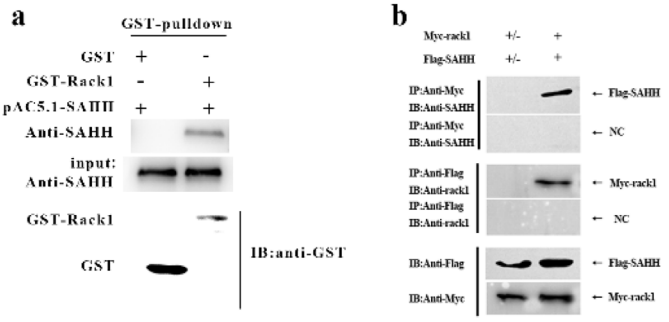

Fig. 6. Interaction between *Lv*SAHH and *Lv*Rack1 *in vitro* (a) and *in vivo* (b).

Rack1 protein Myc-tagged, together with the expression full-length SAHH protein Flag-tagged. Cell lysates were immunoprecipitated with a monoclonal anti-Myc or anti-Flag antibody, and the immunoprecipitated proteins were analyzed by Western blotting using a polyclonal anti-SAHH or the anti-Rack1 antibody, respectively. As

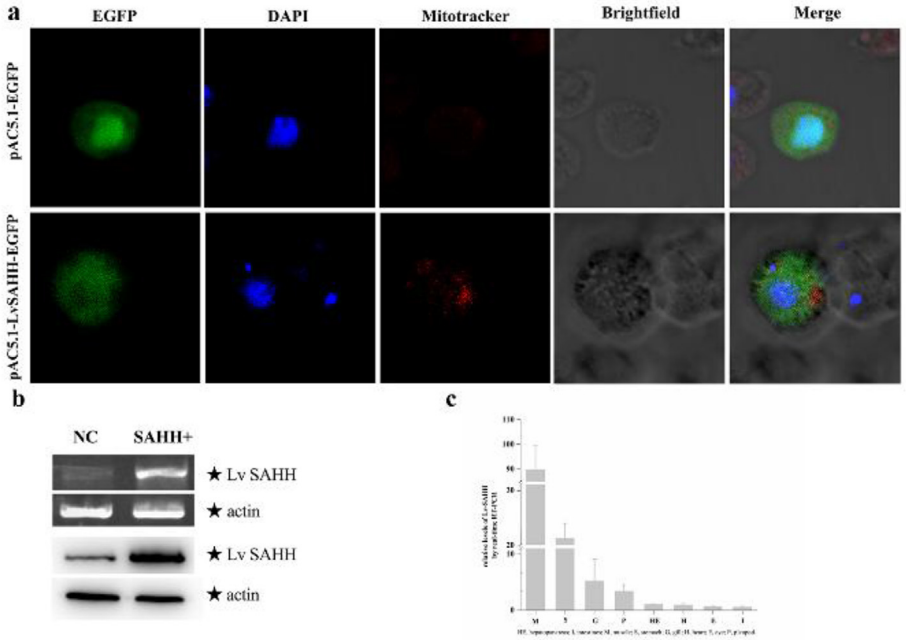

Fig. 5. Subcellular localization and tissue-specific expression of *Lv*SAHH. (a) Subcellular localization of *Lv*SAHH; (b) realtime PCR and western blot detection SAHH overexpression; (c) tissue-specific mRNA expression of the *LvSAHH* determined by quantitative real-time PCR.

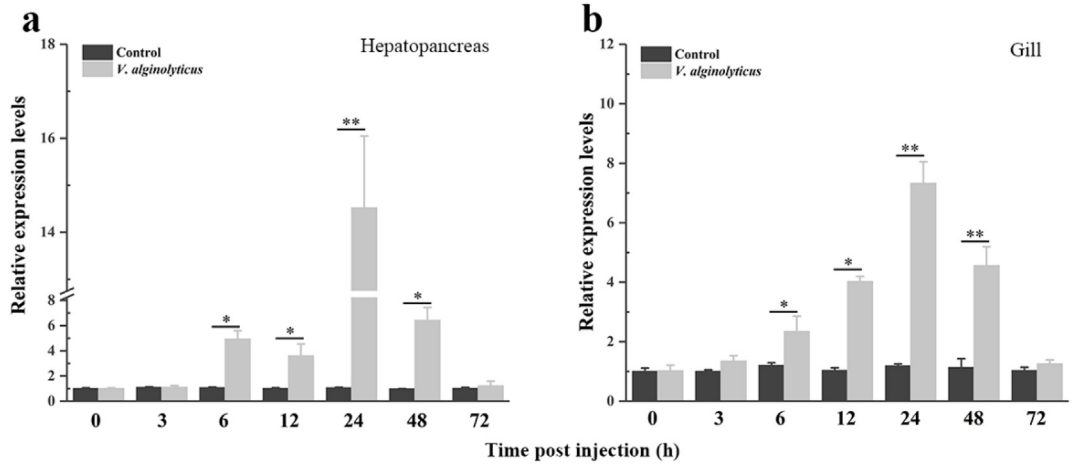

Fig. 7. Expression pattern of *LvSAHH* in hepatopancreas (a) and gill (b) after *Vibrio alginolyticus* injection by quantitative real-time PCR analysis.

shown in Fig. 6b, SAHH is sufficient for the interaction with Rack1.

3.5. Upregulation of LvSAHH in V. alginolyticus infection

To confirm the expression level of *LvSAHH* in different tissue, the *SAHH* profiles was investigated by qPCR, and the results revealed that *LvSAHH* mRNA levels in the hepatopancreas and gill significantly increased about 15-fold and 8-fold after 24 h of infection, then began to decrease, respectively (Fig. 7a and b).

3.6. LvSAHH regulated inflammatory cytokines expression in shrimp

The *LvSAHH* was knocked down (0.45-fold and 0.53-fold compared with *GFP*-RNAi) in shrimp hepatopancreas and gill, respectively (Fig. 8a, g). *LvRack1* (0.22-fold, $p < 0.01$; 0.51-fold, $p < 0.05$), *LvToll1* (0.41-fold, $p < 0.01$; 0.26-fold, $p < 0.01$), *LvToll2* (0.37-fold, $p < 0.01$; 0.29-fold, $p < 0.01$), *LvToll3* (0.44-fold, $p < 0.01$), *LvIL-16* (0.35-fold, $p < 0.01$; 0.28-fold, $p < 0.01$) transcripts in hepatopancreas and gill were decreased significantly in *dsLvSAHH*-injected shrimp at 24 h after *V. alginolyticus* injection compared with that in *dsGFP*-injected shrimp, respectively (Fig. 8 b-f, h-l). There was no significant change in *LvToll3* expression between *dsLvSAHH* -injected and *dsGFP*-injected groups.

4. Discussion

SAHH is a highly conserved tetrameric protein that catalyzes the reversible hydrolysis of AdoHcy to adenosine and Hcy and plays crucial roles in a variety of physiological and pathological processes [9,24]. Recent findings that SAHH deficiency caused clinical manifestations of psychomotor developmental delay, hypomyelination, white matter atrophy, liver dysfunction, and striking tissue accumulation of SAM and SAH [25]. Furthermore, S-adenosyl methionine (AdoMet) increasement promotes oxidative stress and decreases Na^+, K^+-ATPase activity in cerebral cortex of rats [26]. However, the knowledge of how SAHH regulates the gene expression, as well as other target genes such as cytokines is still not very clear in invertebrates. In this study, a full-length cDNA sequence of the SAHH was successfully cloned from *L.*

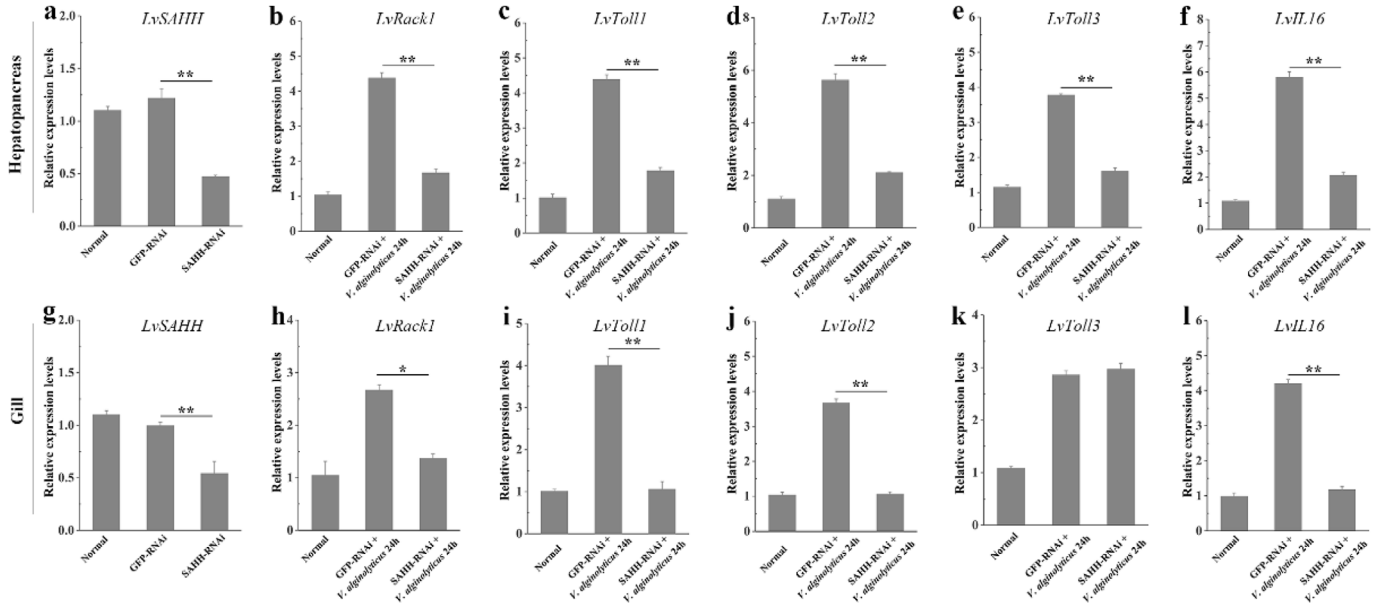

Fig. 8. Gene expression in *LvSAHH* silenced shrimp *Vibrio alginolyticus* injection. The efficiency of *Lv*SAHH-RNAi in hepatopancreas (a) and gill (g) was analyzed by qRT-PCR. After ds*LvSAHH* injection, the expression of *LvRack1*, *LvToll1*, *LvToll2*, *LvToll3*, *LvIL-16* in hepatopancreas (b–f) and gill (h–l) of shrimp at 24 h after *Vibrio alginolyticus* injection was detected by qRT-PCR, respectively. The GFP-RNAi was used as the control. Each value is the mean ± SD. * significantly different ($p < 0.05$) and ** significantly different ($p < 0.01$) without groups (*t*-test).

vannamei. To our knowledge, this is the first full-length cDNA sequence of SAHH cloned from a crustacean. The SAHH gene of *L.vannamei* displays high sequence similarity with known SAHH genes from other organisms (both vertebrate and invertebrate). The significant homology noted between different categorized groups clearly suggests that SAHHs are conserved proteins in almost all species. Previous studies indicate that SAHH is crucial for maintaining the cellular methylation potential, indirectly impacting methylation of DNA, mRNA, tRNA, lipid and protein [2,4]. It is thought to be located at the sites of ongoing AdoMet dependent methylation, presumably in the cell nucleus [24]. Indeed, our results show that endogenous SAHH is located both in cytoplasm and the nucleus, implying the interaction with various proteins.

The cells can be survival in many stresses because they have evolved diverse mechanisms that allow organisms to respond to environmental and physiological stresses. For instance, SAHH is critical for the regulation of the trans-methylation cycle since excess SAH inhibits the methylation reaction [27]. And SAHH can also regulates immune responses such as cellular apoptosis, cell differentiation, tumorigenesis, and cytokine production in vertebrates [10,24,28,29]. Interesting, The Rack1 with seven highly conserved internal consensus Trp-Asp 40 (WD40) repeats family protein, found that involved in diverse processes including apoptosis, proliferation, cell cycle, cell survival, cell adhesion, migration and immune responses [30–32]. Rack1 though interact with protein kinase C involved regulate cell growth, cell death, and stress response [33]. Geijsen et al. demonstrated that Rack1 as a possible adapter molecule associating with the intracellular domain of cytokine receptors [16]. Barbara et al. found that Rack1 can regulate the anti-inflammatory activity of estrogen in glial cells [34]. Further evidence linking Rack1 to immune responsiveness is its involvement in killing the microbial invaders through regulation of superoxide anion generation [35]. In addition, Rack1 is also involved in the NF-kB signaling pathway, suggesting that Rack1 plays an important role in innate immune response. Our results found that SAHH interacted with Rack1 *in vivo* and *in vitro* by CoIP and GST-pulldown, respectively. Previous studies have shown that SAHH genes were differentially expressed in cows of breast after infected by pathogen [36]. It was reported that overexpression SAHH increase Rack1 expression and promoted cell apoptosis, inhibited cell migration and adhesion [28]. In contrast, our study found that silencing SAHH leads to moderate inhibition of Rack1. Further study showed that *LvSAHH* could regulate the TLRs and IL-16 expression in *V. alginolyticus* injection shrimp. These results of *in vivo* studies revealed that *Lv*SAHH by activation Rack1 to regulating the production of cytokines. The immune responses were tissue-specific because hepatopancreas seemed to have a greater ability to defend against pathogens and was more sensitive to stress than gill based on the results of TLRs and IL-16 mRNA expression, hepatopancreas is a major site of toxic metal and bacteria accumulation. These findings would be helpful for understanding the activation mechanism of SAHH as well as its function in regulating the production of cytokines in invertebrates.

Acknowledgments

This research was supported by the National Natural Science Foundation of China (Grant Nos. 31372205 and 31500325), Guangdong province science and technology research spark project (2013B020503060), and the Innovation Project of Graduate School of South China Normal University.

References

[1] G.D. Haba, G. Cantoni, The enzymatic synthesis of S-adenosyl-L-homocysteine from adenosine and homocysteine, J. Bio. Chem. 3 (1959) 603.
[2] V.K.C. Ponnaluri, P.O. Esteve, C.I. Ruse, S. Pradhan, S-adenosylhomocysteine hydrolase participates in DNA methylation inheritance, J. Mol. Biol. 14 (2018) 2051–2065.
[3] H. Richards, P. Chiang, G. Cantoni, Adenosylhomocysteine hydrolase. Crystallization of the purified enzyme and its properties, J. Bio. Chem. 12 (1978) 4476.
[4] Y. Kusakabe, M. Ishihara, T. Umeda, D. Kuroda, M. Nakanishi, Y. Kitade, et al., Structural insights into the reaction mechanism of S-adenosyl-L-homocysteine hydrolase, Sci. Rep. 5 (2015) 16641.
[5] A. Banerjee, 5'-terminal cap structure in eucaryotic messenger ribonucleic acids, Microbiol. Mol. Biol. R. 2 (1980) 175.
[6] P. Ueland, A. Svardal, H. Refsum, J. Lillehaug, J. Schanche, S. Helland, Disposition of endogenous S-adenosylhomocysteine and homocysteine following exposure to nucleoside analogues and methotrexate, Biol. Methylation Drug Des. (1986) 263–274.
[7] P.K. Chiang, R.K. Gordon, J. Tal, G.C. Zeng, B.P. Doctor, et al., S-adenosylmethionine and methylation, FASEB J. 4 (1996) 471–480.
[8] V. Cowling, Regulation of mRNA cap methylation, Biochem. J. 2 (2010) 295.
[9] Z.M. Lin, M. Ma, H. Li, Q. Qi, Y.T. Liu, et al., Topical administration of reversible SAHH inhibitor ameliorates imiquimod-induced psoriasis-like skin lesions in mice via suppression of TNF-alpha/IFN-gamma-induced inflammatory response in keratinocytes and T cell-derived IL-17, Pharmacol. Res. 129 (2018) 443–452.
[10] Q.L. Wu, Y.F. Fu, W.L. Zhou, J.X. Wang, Y.H. Feng, et al., Inhibition of S-adenosyl-L-homocysteine hydrolase induces immunosuppression, J. Pharmacol. Exp. Ther. 2 (2005) 705–711.
[11] B. Lemaitre, J. Hoffmann, The host defense of *Drosophila melanogaster*, Annu. Rev. Immunol. 25 (2007) 697–743.
[12] H.C. Wang, C.W. Tseng, H.Y. Lin, I.T. Chen, Y.H. Chen, et al., RNAi knock-down of the *Litopenaeus vannamei* Toll gene (LvToll) significantly increases mortality and reduces bacterial clearance after challenge with *Vibrio harveyi*, Dev. Comp. Immunol. 1 (2010) 49–58.
[13] T. Mekata, T. Kono, T. Yoshida, M. Sakai, T. Itami, Identification of cDNA encoding Toll receptor, MjToll gene from kuruma shrimp, *Marsupenaeus japonicus*, Fish Shellfish Immunol. 1 (2008) 122–133.
[14] C.J. Yang, J.Q. Zhang, F.H. Li, H.M. Ma, Q.L. Zhang, et al., A toll receptor from Chinese shrimp *Fenneropenaeus chinensis* is responsive to *Vibrio anguillarum* infection, Fish Shellfish Immunol. 5 (2008) 564–574.
[15] J. Chen, J. Liu, S. Xiao, Z. Yu, Molecular cloning, characterization and expression analysis of receptor for activated C kinase 1 (RACK1) from pearl oyster (*Pinctada martensii*) challenged with bacteria and exposed to cadmium, Fish Shellfish Immunol. 6 (2011) 781–787.
[16] N. Geijsen, M. Spaargaren, J.A. Raaijmakers, J.W. Lammers, L. Koenderman, P.J. Coffer, Association of Rack1 and PKCbeta with the common beta-chain of the IL-5/IL-3/GM-CSF receptor, Oncogene 36 (1999) 5126–5130.
[17] M. Colonna, A. Krug, M. Cella, Interferon-producing cells: on the front line in immune responses against pathogens, Curr. Opin. Immunol. 3 (2002) 373–379.
[18] S.P. Yeh, Y.N. Chen, S.L. Hsieh, W.T. Cheng, C.H. Liu, Immune response of white shrimp, *Litopenaeus vannamei*, after a concurrent infection with white spot syndrome virus and infectious hypodermal and hematopoietic necrosis virus, Fish Shellfish Immunol. 4 (2009) 582–588.
[19] T. Peng, M.M. Gu, C.S. Zhao, W.N. Wang, M.Z. Huang, et al., The GRIM-19 plays a vital role in shrimps' responses to *Vibrio alginolyticus*, Fish Shellfish Immunol. 49 (2016) 34–44.
[20] G.H. Cha, W.N. Wang, T. Peng, M.Z. Huang, Y. Liu, A Rac1 GTPase is a critical factor in the immune response of shrimp (*Litopenaeus vannamei*) to *Vibrio alginolyticus* infection, Dev. Comp. Immunol. 2 (2015) 226–237.
[21] J. Qiu, W.N. Wang, L.J. Wang, Y.F. Liu, A.L. Wang, Oxidative stress, DNA damage and osmolality in the Pacific white shrimp, *Litopenaeus vannamei* exposed to acute low temperature stress, Toxicol. Pharmacol.: CBP 1 (2011) 36–41.
[22] Q.L. Feng, K.G. Davey, A.S.D. Pang, M. Primavera, T.R. Ladd, et al., Glutathione S-transferase from the spruce budworm, *Choristoneura fumiferana*: identification, characterization, localization, cDNA cloning, and expression, Insect. Biochem. Molec. 9 (1999) 779–793.
[23] M. Mourtacla-Maarabouni, L. Kirkham, F. Farzaneh, G.T. Williams, Functional expression cloning reveals a central role for the receptor for activated protein kinase C 1 (Rack1) in T cell apoptosis, J. Leukoc. Biol. 2 (2005) 503–514.
[24] I. Grbesa, A. Kalo, R. Beluzic, L. Kovacevic, A. Lepur, F. Rokic, et al., Mutations in S-adenosylhomocysteine hydrolase (AHCY) affect its nucleocytoplasmic distribution and capability to interact with S-adenosylhomocysteine hydrolase-like 1 protein, Eur. J. Cell Biol. 6 (2017) 579–590.
[25] T. Honzik, M. Magner, J. Krijt, J. Sokolova, O. Vugrek, et al., Clinical picture of S-adenosylhomocysteine hydrolase deficiency resembles phosphomannomutase 2 deficiency, Mol. Genet. Metab. 3 (2012) 611–613.
[26] A. Zanatta, C. Cecatto, R.T. Ribeiro, A.U. Amaral, A.T. Wyse, et al., S-adenosylmethionine promotes oxidative stress and decreases Na(+), K(+)-ATPase activity in cerebral cortex supernatants of adolescent rats: implications for the pathogenesis of S-adenosylhomocysteine hydrolase deficiency, Mol. Neurobiol. 7 (2018) 5868–5878.
[27] I. Baric, C. Staufner, P. Augoustides-Savvopoulou, Y.H. Chien, D. Dobbelaere, et al., Consensus recommendations for the diagnosis, treatment and follow-up of inherited methylation disorders, J. Inherit. Metab. Dis. 1 (2017) 5–20.
[28] Q. Li, L. Mao, R. Wang, L. Zhu, L. Xue, Overexpression of S-adenosylhomocysteine hydrolase (SAHH) in esophageal squamous cell carcinoma (ESCC) cell lines: effects on apoptosis, migration and adhesion of cells, Mol. Bio. Rep. 4 (2014) 2409–2417.
[29] J.F. Leal, I. Ferrer, C. Blanco-Aparicio, J. Hernandez-Losa, Y.C.S. Ramon, et al., S-adenosylhomocysteine hydrolase downregulation contributes to tumorigenesis, Carcinogenesis 11 (2008) 2089–2095.
[30] D.R. Adams, D. Ron, P.A. Kiely, RACK1, A multifaceted scaffolding protein: structure and function, Cell Commun. Signal. 9 (2011) 22.
[31] J.J. Li, D. Xie, RACK1, a versatile hub in cancer, Oncogene 15 (2015) 1890–1898.

[32] N. Waiskopf, K. Ofek, A. Gilboa-Geffen, U. Bekenstein, A. Bahat, et al., AChE and RACK1 promote the anti-inflammatory properties of fluoxetine, J. Mol. Neurosci.: MN 3 (2014) 306–315.
[33] R. Gopalakrishna, S. Jaken, Protein kinase C signaling and oxidative stress, Free Radic. Bio. Med. 9 (2000) 1349–1361.
[34] B. Viviani, E. Corsini, M. Binaglia, L. Lucchi, C.L. Galli, M. Marinovich, The anti-inflammatory activity of estrogen in glial cells is regulated by the PKC-anchoring protein RACK-1, J. Neurochem. 5 (2002) 1180–1187.
[35] H.M. Korchak, L.E. Kilpatrick, Roles for beta II-protein kinase C and RACK1 in positive and negative signaling for superoxide anion generation in differentiated HL60 cells, J. Bio. Chem. 12 (2001) 8910–8917.
[36] M. Schwerin, D. Czernek-Schafer, T. Goldammer, S.R. Kata, J.E. Womack, et al., Application of disease-associated differentially expressed genes-Mining for functional candidate genes for mastitis resistance in cattle, Genet. Sel. Evol. 35 (2003) 19–34.